

# Experimental Study of Temperature Distribution and Flame Spread Over an Inert Porous Bed Wetted with Liquid Fuel

J. Zanganeh and B. Moghtaderi<sup>1</sup>

Priority Research Centre for Energy, Chemical Engineering, School of Engineering,  
Faculty of Engineering & Built Environment, The University of Newcastle,  
Callaghan, NSW 2308, Australia  
Jafar.Zanganeh@uon.edu.au  
Behdad.Moghtaderi@Newcastle.edu.au

## ABSTRACT

A combined experimental and modelling study was carried out to investigate the flame spread phenomenon over a porous bed wetted with finite quantity of super-flash liquid fuel. Measurements included flame spread rate, temperature distribution, and visual observation. Sand particles ranging from 0.5 to 5 mm and Propanol (flash point 12 °C) were used as porous bed and liquid fuel, respectively.

Results corresponding to the rate of flame spread show that regardless of airflow speed and/or direction the rate of flame spread decreases as either the bed depth or particle size increases, however the flame spread deceleration rate is more distinct under opposed airflow.

Temperature measurements and mathematical modelling results indicated the existences of three different temperature regions in the bed. The magnitude of temperature in upper region was significantly larger than those of the lower region. The modelling results were in good agreement with the experimental data.

**Keywords:** Flame spread, Liquid fuel, Porous bed, Temperature distribution, Assisted and Opposed airflow.

## Nomenclature

$c$	Thickness of vapour-solid region
$\Delta c$	Thickness of three-phase region
$d$	Diameter of solid particle
$\Delta h_{vap}$	Latent heat of evaporation
$T$	Temperature
$F_c$	Capillary force
$T_s$	Surface temperature
$T_l$	Liquid temperature
$V_f$	Flame spread rate
$x, y$	Cartesian coordinates
$K$	Permeability
$T_\infty$	Initial temperature
$T_b$	Boiling temperature of liquid

## Greek Symbols

$\alpha$	Thermal diffusivity
$\lambda$	Thermal conductivity
$\rho$	Density
$\pi$	Mathematical constant

---

<sup>1</sup>Corresponding author: Phone:+61(2)4985-4411, Fax: +61(2)4921-6893, Email: Behdad.Moghtaderi@Newcastle.edu.au

**Subscripts**

<i>liq</i>	Liquid
<i>vap</i>	Vapour
<i>l</i>	Liquid solid region
<i>v</i>	Vapour solid region
<i>t.ph</i>	Three-phase region

**INTRODUCTION**

Accidental fires in industrial settings often involved the spillage of combustible liquids over porous beds of concrete, soil and sand. In the presence of an ignition source, the liquid fuel may get ignited and lead to stable flame, which in turn may spread over the porous bed.

The characteristics of the flame spread phenomenon, in such cases, are considerably different from those of non porous solids such as PMMA or liquid pools. The intensity and scale of fires over porous beds is extremely depends upon the liquid fuel flash point and characteristics of porous bed such as pore volume, pore size distribution and primary temperature [1].

Despite the importance of flame spread over porous beds, only a limited number of studies are available on the subject in the open literature [1–13]. There are, however many papers on pool fires as reported in Refs. 2 and 3. Ishida [4–8], Takeno and Hirano [9, 10], Takeuchi et al [11], Suzuki [12–14], Chao [1] and Wang [15] performed broad experimental studies of the flame spread over glass, sand and steel beads filled up with liquid fuel. They found that the flame spread rate is dramatically depends upon the particle size [4, 10]. In addition it has been declared that the rate of flame spread is generally slower over porous bed when compared with pool fires [5, 9]. The temperature of porous bed is considered as an affective parameter on the rate of flame spread.

It is believed that conduction is the main mode of heat transfer from the flame into the porous bed and fuel [1, 4, 5, 10, 11, 16, and 17]. However, convection and radiation become more important by transferring heat from the flame to the unburned areas. When an unburned bed surface becomes sufficiently hot, extra heat vaporizes the fuel. The resulting gaseous fuel gradually comes up into contact with ambient oxygen at the surface and consequently increases the flame spread speed [6]. For example studies by Ishida [5, 6] have shown that the rate of flame spread increases with increasing of the bed temperature and this phenomenon is much pronounced when the bed temperature is much higher than the liquid fuel flash point.

The flame spread rate as well as its behaviour is significantly affected by the availability of fuel at the combustion zone and continuous fuel supply to this region. Therefore for beds with sufficient fuel supply (i.e. flushed bed) the flame spreads faster compared with beds of insufficient fuel supply (i.e. unflushed bed). In the case of flushed beds due to the existence of large quantity of liquid fuel, flame propagation speed and behaviour is very similar to the pool fire, also the flame can sustain for longer period of time.

The majority of the previous studies have almost exclusively focused on scenarios where unlimited fuel supply was available, while in practical situations involving accidental fuel spillage, the porous bed is not always soaked with the fuel since the ratio of the fuel to the porous bed is relatively small. As a result, the finite quantity of the liquid fuel in this case would certainly have dramatic impact on the flame, altering its propagation behaviour and/or characteristics. We have shown in previous studies [18, 19] that in the case of sand beds wetted with finite quantities of liquid fuel, the flame spread rate substantially decreases as the particle sizes are increased. Also, deeper sand beds gradually lead to slower flame spread. Regardless of importance of flame spread under such conditions (finite fuel supply) it is still not well understood. The present paper build on our previous works [18,19, and 28] and attempt to shed more light on the flame spread phenomenon over porous beds wetted with finite quantities of liquid fuel.

The aims of this study are to investigate in details: (1) the relationship between the physical properties of the porous bed and the flame spread rate; (2) the temperature distribution inside the porous bed during the combustion process; and (3) the physical features of flame spread under various operating conditions.

To achieve the broad objective of the study a comprehensive series of combined experimental and theoretical investigations were carried out. The details of these are discussed below.

## EXPERIMENTAL SETUP AND TECHNIQUES

A series of laboratory scale experiments were performed and the schematic view of the experimental setup can be seen in Figure 1.

A scaled channel was designed to mimic the spread of flames over a range of porous media under realistic conditions within a controlled laboratory setting (Figure 1). The  $1.5 \times 0.08 \times 0.04$  m channel was made out of stainless steel. The channel was mounted on a manual jack so that the

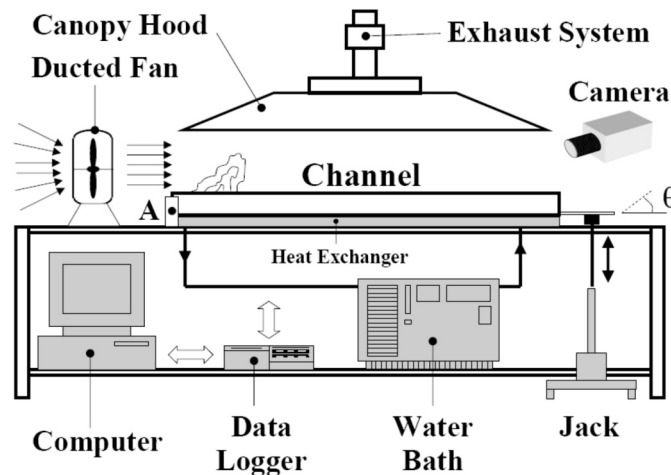


Figure 1. Schematic diagram of experimental set up.

inclination angle of the channel can be varied. The channel was also equipped with a cooling and heating system connected to a water bath located beneath the channel. The external surfaces of the channel were covered with a 5 mm thick insulating material to prevent heat losses. The channel was filled with 6 different particle sizes with median diameters of 0.5, 1, 2, 3, 4 and 5 mm,  $\rho = 2680 \text{ kg/m}^3$  as porous bed. In this study, the different particle sizes were obtained by utilising corresponding sieves in a sieve shaker machine. Three different depths (13.3, 26.6 and 39.9 mm) were selected to investigate the effects of the bed depths on the flame spread phenomenon and combustion characteristics.

A ducted fan with a  $0.2 \times 0.2$  m outlet connected to a speed controller was used to simulate the effect of air stream on the flame spread. Furthermore a telescopic anemometer was used to map the air stream over the bed. A high speed video Camera and an accurate stopwatch were used to measure the flame speed. The airflow velocity could be adjusted over a range between 0 and 2 m/s. A canopy hood installed above the bed and connected to an exhaust fan to extract the smoke out of the laboratory.

Propanol (boiling point  $82.4 \text{ }^\circ\text{C}$  and flash point  $12 \text{ }^\circ\text{C}$ ) was used as the liquid fuel in all experiments. The fuel was uniformly distributed by a fuel liquid distributor all over the porous bed. The ratio of fuel volume to the sands weight in all experiments was kept at 0.1 L/kg (fuel volume/sand weight).

Ignition was achieved using a pilot flame placed near the end of the channel depending upon the particular airflow direction. The flame speed and hence the spread rate were digitally determined from high-speed video cinematography, video image processing as well as visual observation.

A thermocouple grid was designed and installed inside the channel to measure the temperature distribution in porous bed. The grid was connected to the data acquisition and a computer. The embedded grid consisted of 24 K type thermocouples (Ni/Chr – Ni/Al,  $-200 - 1370 \text{ }^\circ\text{C}$ ) all with a sheath diameter of 1 mm. The thermocouples were introduced from one of the side walls of the channel and were arranged in 8 columns and three rows with 0.2 m interval between columns and 13.3 mm distance between alternative rows (see Figure 2).

## Experimental Study of Temperature Distribution and Flame Spread Over an Inert Porous Bed Wetted with Liquid Fuel

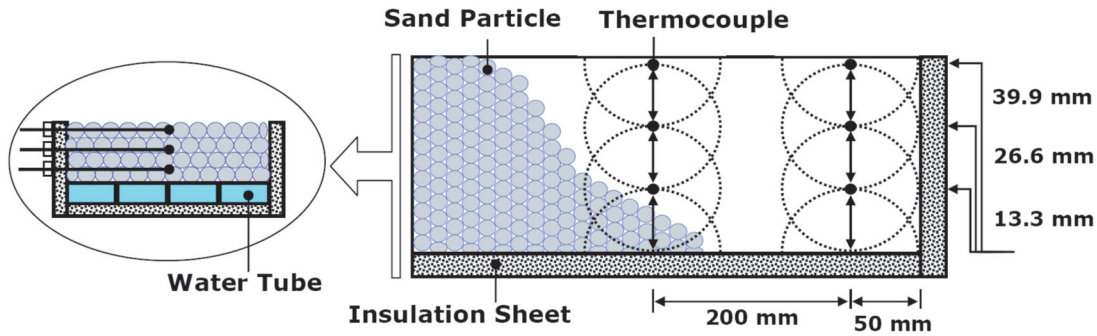


Figure 2. The channel side view and thermocouples location.

A heating-cooling water bath (equipped with a circulation system and fitted with a digital controller) was connected to a grid of tubes embedded underneath the channel to maintain the temperature of the bottom of the channel around the ambient temperature. In order to decrease the effect of ambient temperature on the thermocouple reading, thermocouples were embedded just beneath the surface ( $y = -1$  mm). This was the nearest distance to the bed surface.

All experiments were conducted at ambient temperature of about 25 °C. At the beginning of each experiment all thermocouples were calibrated with a standard *J* type thermocouple to make sure they were in correct working order. Afterward the channel was filled with sand particles to a certain depth according to the experimental plan. The surface of the bed was smoothed out using a trowel to make the surface as even as possible without any compaction. At this stage the ducted fan was turned on in the case of assisted or opposed airflow configurations.

The liquid fuel was distributed uniformly all over the bed using a fuel distributor system developed in our laboratory as part of this study. After a pause period, the fuel was ignited using a gas pilot igniter and flame was let to spread along the length of the bed. The progress was captured digitally using the height speed video camera.

### MATHEMATICAL MODELING

When a flame front spreads over a porous bed wetted with liquid fuel, the temperature of the fuel inside the bed quickly rises due to the heat transfer from the flame. This leads to formation of a fuel vapour which diffuses out of the bed and reacts with the air in the boundary layer surrounding the bed ultimately assisting the flame front to propagate over the porous bed.

In order to describe the above phenomena and determine the temperature distribution in the bed we adopted the mathematical model developed by Kuwana and co-workers [17]. The model considers the physical configuration depicted schematically in Figure 3. The model has been formulated based on the following assumptions:

- The coordinate system is fixed at the flame leading edge the fuel moves at the velocity of  $V_f$  in the opposite direction to the flame.
- The fuel movement in the porous bed due to the flame spread is simulated using thermal boundary conditions at the surface of the fuel soaked bed, as adopted in the previous studies [17, 25–27].
- The process is assumed to be steady-state.
- The fuel soaked porous bed consists of three regions (see Figure 13), namely: vapour, three-phase, and liquid regions.
- The interfaces between the adjacent regions are of parabolic shape.
- Recession of the fuel level due to evaporation is neglected.
- The temperature of the lower boundary of the liquid fuel region remains at initial temperature, and the temperature of the three-phase region remains at the liquid fuel boiling point.
- The thermo-physical properties of all three regions are assumed to be constant.
- The temperature of the upper surface of the bed remains constant during the flame spread and heat transfer to the fuel via radiation and convection are neglected.
- The surface layer ahead of the flame is assumed to be adiabatic.

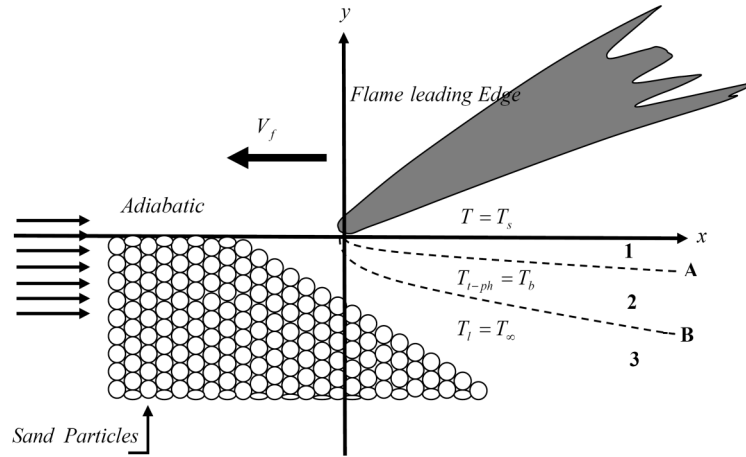


Figure 3. Schematic diagram of flame spread leading edge and different fuel phase regions; 1) vapour region; 2) three phase region; and 3) liquid region. A) vapour interface; B) liquid interface (adapted from [17]).

Based on the above assumptions and following a series of mathematical manipulation, it can be shown that under steady-state conditions the relationship between the flame spread rate (i.e. velocity of flame front) and controlling parameters such as boundary temperatures and thermo-physical properties can be expressed by the following equation:

$$\lambda \sqrt{\frac{2V_f}{\pi(c + \Delta c)\alpha_l}} \frac{T_b - T_\infty}{\operatorname{erf}\left(\frac{\sqrt{V_f(c + \Delta c)}}{2\alpha_l}\right)} \exp\left\{-\frac{V_f(c + \Delta c)}{2\alpha_l}\right\} + \varepsilon \rho_{liq} V_f \Delta h_{vap} = \lambda_v \sqrt{\frac{2V_f}{\pi c \alpha_v}} \frac{T_s - T_b}{\operatorname{erf}\left(\frac{\sqrt{V_f c}}{2\alpha_v}\right)} \exp\left(-\frac{V_f c}{2\alpha_v}\right) \quad (1)$$

Table 1 summarises the values of all parameters employed in this study to solve equation 1.

**Table1: Parameters used in this study**

Parameter	Value	Parameter	Value
$T_\infty$	298 k	$\rho_{liq}$	790 kg/m <sup>3</sup>
$T_b$	355 k	$\alpha_l$	$1.95 \times 10^{-5}$ m <sup>2</sup> /s
$T_s$	610 k	$\alpha_v$	$3.48 \times 10^{-3}$ m <sup>2</sup> /s
$\lambda_l$	0.1446 w/mk	$c$	$1 \times 10^{-8}$ m
$\lambda_v$	0.01082 w/mk	$\Delta c$	$1 \times 10^{-7}$ m
$V_f$	0.8–1.75 m	$\varepsilon$	0.35 – 0.6
$\Delta h_{vap}$	651 kJ/kg	$\pi$	3.14

## RESULTS AND DISCUSSION

### Visual Observations

Experimental results obtained in this study for the flame characteristics, temperature distribution and flame spread rate over porous sand beds in horizontal orientation under various airflow configurations are shown in Figures 4 to 14.

Results corresponding to the flame characteristics obtained by digital cinematography showed that the flame leading edge consists of blue colour followed by a luminous yellow zone. These observations

## Experimental Study of Temperature Distribution and Flame Spread Over an Inert Porous Bed Wetted with Liquid Fuel

are nearly similar to features observed by Ishida, and Kong et al [4, 16], although the blue flame region is not seen clearly on the photographs as the flame spread was very fast. In the luminous yellow zone just behind the blue flame region, a few pairs of longitudinal vortexes are generally observed.

The flame luminance colour depends generally on the construction of chemical fuel and the way that combustion process is taking place. The chemical features are very much related to the supplementation of fuel and oxygen. At the beginning of combustion process due to the availability of sufficient oxygen, the combustion is completed; hence, the flame colour is blue. Also the blue colour addresses that there is no soot formation and emission from the flame. The flame characteristics were very similar in all experiments. The relative size and the extent of the blue leading edge in quiescent and airflow conditions are quite different influencing the heat transfer mechanisms and thereby the overall flame spread rate.

Figures 4 to 7 are typical images of the flame which occurs instantly after flame spread upon the sand bed. As combustion continued, the flame size became bigger and its height slowly rose up until the flame shape was almost conical. Figure 4 shows the flame aspects in quiescent condition. Since there is no airflow the condition remain steady. In this situation the flame burns monotonically in conical shape.

Figures 5 to 7 illustrate the flame configuration under assisted airflow. As shown the airflow disturbs the steady state condition, in turn, deformation of flame configuration. As the airflow increases the flame takes a wavier shape with more broken external envelop in compare with the flame envelop under no airflow condition. As it is observed, under airflow condition flame tilted down and approaches the sand bed. It is believed that when the flame approaches the surface, it helps preheating unburnt surface which is located at the front of the flame leading edge. As such the flame spreads faster.

The flame aspects in these figures (Figures 4 to 7) clearly show the alteration of the flame height under airflow conditions. As shown, the flame spread height decreases as the airflow speed increases. Compared with the flame spread under airflow condition, the flame height is significantly higher under no airflow condition. The flame height for the quiescent condition was measured around 0.3 m. which is approximately 3 times higher when compared with the flame height under 1.5 m/s airflow speed. However with respect to the time the flame size and height became smaller and shorter, respectively. The flame then gradually started a series of continuous flickering. The flickering changed from non stop to very slow alternative mode. Then the flame totally vanished.

Compared with quiescent condition under airflow condition flame covers more surface, thereby more heat is transferred to the adjacent areas. From point of fire safety view, the importance of this feature becomes more pronounced when flame happens in a roofed corridor or stock with natural or artificial ventilation. Most of stocks are usually built with height level roof to embed more stuff in. On the other hand fire safety systems such as fire alarms, sensors and sprinklers more often are installed underneath the roof. Therefore if an unwanted flame happens, due to the fuel spillage, in a stock with free stream airflow, flame spreads faster everywhere. Moreover due to the less soot formation and short flame pillars at this stage the reaction of fire safety systems may become slower. However further investigations need to be done at this particular area.



Figure 4. Flame spread in quiescent condition  $U = 0$ ,  $\theta = 0^\circ$ .



Figure 5. Flame spread under airflow condition for  $U = 0.5$  m/s,  $\theta = 0^\circ$ .



Figure 6. Flame spread under airflow condition for  $U = 1 \text{ m/s}$ ,  $\theta = 0^\circ$ .



Figure 7. Flame spread under airflow condition for  $U = 1.5 \text{ m/s}$ ,  $\theta = 0^\circ$ .

### Flame Spread Measurements

Figures 8 to 10 illustrate bar charts of the flame spread rate over different particle sizes ranging from 0.5 to 5 mm as a function of bed depth under different airflow conditions.

As shown in Figure 8, in quiescent condition (i.e. no airflow) the flame spread rate decreases as the particle size increases. The highest flame spread rate is about 1.7 m/s corresponds to the shallowest bed (13.3 mm) contains the finest particle size (0.5 mm). The flame spread rate for the same particle size drops to 1.44 m/s and 1.2 m/s as the bed depth increases to 26.6 mm and 39.9 mm, respectively. It is observed that the flame spread rate almost decreases linearly with an almost constant rate (around 15% with doubling the bed depth). For coarse particles (5 mm) the flame spread rate is around 1.4 m/s for bed depth of 13.3 mm. A drop of almost 19% when compared with the flame spread over fine particles (0.5 mm) in an identical situation.

A similar drop in the rate of flame spread is observed when the flame occurs under the assisted or opposed airflow conditions as indicated in Figures 9 and 10, respectively. In these figures the flame spread rate is plotted versus particle sizes. The assisted and opposed airflow speed for these beds are identical equal to 1 m/s. As observed, regardless of airflow direction the flame spread rate corresponds to a given particle size increases as the bed depth decreases, although the deceleration rate is more pronounced under opposed airflow configuration. Figures 9 and 10 indicates that the rate of

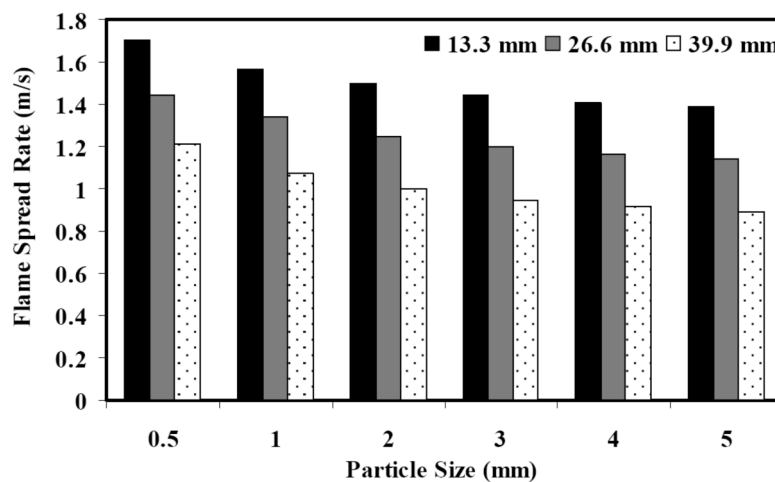


Figure 8. Flame spread rate over various bed depths containing sand particles ranging from 0.5 to 5 mm in quiescent condition and horizontal orientation.

### Experimental Study of Temperature Distribution and Flame Spread Over an Inert Porous Bed Wetted with Liquid Fuel

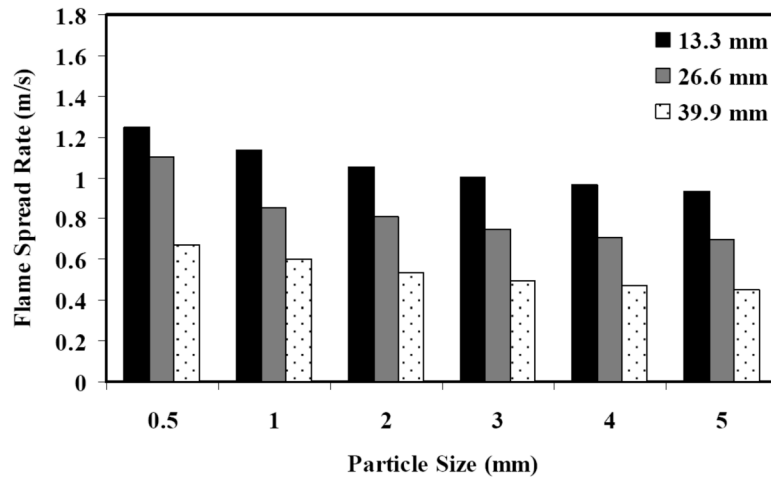


Figure 9. Flame spread rate over various bed depths containing sand particles ranging from 0.5 to 5 mm under assisted airflow (1 m/s) in horizontal orientation.

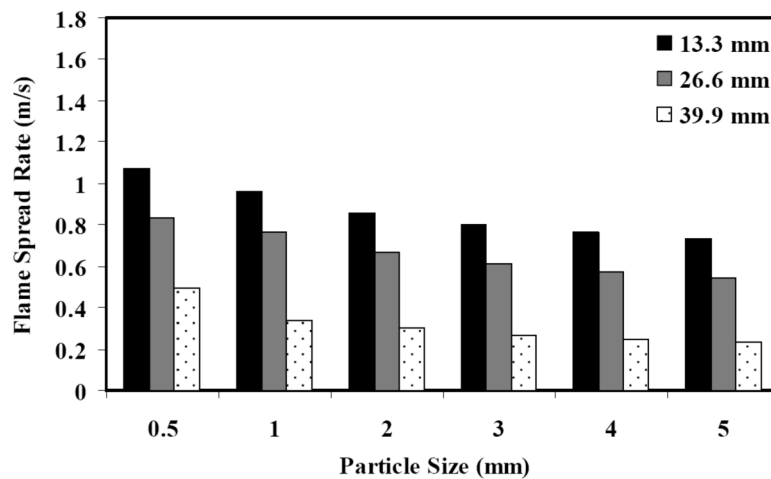


Figure 10. Flame spread rate over various bed depths containing sand particles ranging from 0.5 to 5 mm under opposed airflow (1 m/s) and horizontal orientation.

flame spread for a bed of 13.3 mm depth contains particle size of 0.5 mm declines significantly from 1.25 m/s to 1.07 m/s under 1 m/s assisted and opposed airflow condition, respectively. Evidently the drop in the rate of flame spread for coarser particles and also deeper bed is greater. For example, the flame spread over 5 mm bed particles under assisted airflow decreases from 0.94 m/s to 0.7 and 0.45 m/s as the depths of beds are doubled and tripled, respectively. Compared with the opposed airflow which having the slowest spread rate under otherwise identical conditions. In our study, it was observed for any given particle size, the minimum flame spread rate corresponded to deepest bed under opposed airflow conditions (Figure 10).

Figures 8 to 10 evidently show that apart from the effects of airflow on the rate of flame spread when a finite quantity of liquid fuel is available the rate of flame spread along the surface of an inert porous bed decreases as either the particle sizes or the bed depth are increased. This is an obvious distinction with flame spread over beds which have completely saturated with fuel [12–14].

For instance studies by Murphy [20] and Ishida [5, 6] have indicated that the flame propagation behaviour and flame spread rate over glass bead beds soaked totally with n-octane and methanol are very similar to the pool fires. They examined the rate of flame spread under no airflow configuration was about 1–2 m/sec [5, 6, 20]. The obtained results in this study are agree very well with the results stated by Murphy and Ishida. However they are in contrary with the results expressed by Takeno and Hirano [10]. Takeno and Hirano showed that the rate of flame spread decreases as the particle size

increases until it reaches to a critical point corresponds to a certain particle size (2 mm in their study). Beyond this critical point the rate of flame spread increases as the particle size increases and it attains to the maximum value corresponds to the coarser particle size. Our results do not show such flame spread behaviour, and also no critical particle size or inflection was observed in our flame spread trends.

The relationship among the flame spread rate, particle size, bed depth and the quantity of liquid fuel in this study can be greatly explained applying the concept of capillary rise effect. The capillary rise effect expressed as a force acts in upward direction and conveys the fluid from high concentration region to low concentration region through a capillary channel. This force largely affected by the characteristics of liquid and solid phases. In addition it is directly depends on the contact angle between liquid and solid surface [21].

The capillary rise effect for a particular liquid travelling through a capillary tube has the maximum speed when the contact angle between fluid and solid surface is zero. In the case of fluid flow through a porous bed regardless of contact angle, the particle size and permeability of porous bed also significantly impact on the capillary rise. As expressed in Equation 2 the capillary rise is inversely proportional to the diameter of particle size and porous bed permeability root.

$$F_c \propto \frac{1}{d} \propto \frac{1}{\sqrt{K}} \quad (2)$$

As noted above, in the case of flame spread over porous bed with limited supply of liquid fuel the capillary rise effect plays an important role to transfer the liquid and vapour from the porous bed to the surface at which combustion process takes place. Therefore from the above equation one can infer that the finer beds have larger capillary rise, resulting to the availability of more fuel at the surface. The configuration of porous bed (capillary channels) also dramatically impact on the capillary rise effect.

In general the flame spread lag is attributed to the fuel shortage at the combustion zone. When a porous bed soaked with unlimited fuel supply there is no fuel shortage at the early stages of flame spread and combustion, as such, the capillary rise is not that significant. Whereas for the bed with limited fuel supply, due to the gravity acceleration, fuel gradually penetrates into the bed and pools at the bottom. As a result the fuel concentration gradient at lower regions is relatively higher when compared with upper regions. Therefore for these types of beds the capillary rise acts like a wick and conduct the fuel from lower regions to the surface.

On the other hand during the formation of a porous bed some capillary channels formed inside the bed. Compared with coarse beds, porous beds consisted of fine particles have larger numbers of these capillary channels, however, smaller in diameter. It means that capillary channels which have formed from the fine particles have almost smoother internal surface. This unique property decreases the contact angle between the liquid fuel and the surface of capillary channel. As such, in fine channels the fuel is moved to the surface quite faster. This effect is multiplied by the number of existed capillary channels in each porous bed.

Unlike beds packed with fine particles, in coarse beds the rate of flame spread is slower partly because of the fuel shortage supply. The capillary rise in such beds is less as well; hence fuel supply from the deeper regions within the bed to the surface become slower. This phenomenon becomes more pronounced as the particle size increases. Due to this, only a very thin and diluted layer of gaseous fuel can be formed over the bed resulting in a relatively low flame spread rate. Furthermore because of slowness in the ray of flame spread, less heat can be transferred through the flame leading edge to the unheated regions ahead of the flame. This leads to less fuel evaporation and consequently a further decrease in the rate of the flame spread.

Apart from the capillary rise effect, heat transfer from the flame into the bed and particularly to the liquid fuel also pointed as an affective parameter on the flame spread. As flame leading edge moves upon the bed heat is transferred to the unburnt areas which increase the bed temperature in exterior and interior regions. This preheating phenomenon leads to increase in the fuel evaporation rate, in turn; more gaseous fuel diffuses to the surface and mixed with air somewhere ahead of the flame leading edge. This gaseous fuel increases the combustion reaction and consequently swift the flame spread speed over the pre-heated and unburnt bed.

Similar patterns are observed when flame is spread over a porous bed under assisted and opposed airflow configurations. The airflow affects the flame spread rate with blowing off the gaseous layers from top of the bed surface. The flame spread rate slows down as the airflow speed is increased. In the

case of flame spread under assisted airflow condition, though gaseous layer is pushed-off from the ignition point, the airflow helps heat to be transferred by convection to unburnt areas partly compensating the effect of blow-off. In contrary, under opposed airflow configuration the heat transfer process cannot be easily assisted by the airflow. This effect together with the blow-off (gas thinning) causes the rates of flame spread under opposed flow conditions to be much lower than their assisted airflow counterparts.

Out of all liquid fuel properties, undoubtedly flash point can be nominated as the most important affective factor on the rate of flame spread. Liquids with flashpoint temperature lower than ambient (typical ambient temperature is about 25 °C) usually named super-flash, and fuels with higher flashpoint rather ambient named sub-flash fuels. Therefore in the ambient temperature the fuel evaporation rate for beds soaked with super flash fuels is dramatically higher when compared with sub flash fuels. As such more flammable gas would diffuse to the surface of porous bed. This consequently increases the rate of flame spread. In this study we used propanol flashpoint (12 °C) which is classified as super flash liquid fuel. The swift flame spread in this study can be attributed to the liquid fuel flash point and the high fuel evaporation rate. For example studies by Hirano, Ishida and Takeno [4, 7, 10] have shown that the flame spread rate for sub flash liquid fuel (n-Decan 48 °C) is between 5 – 60 mm/sec. Similar results for Kerosene (50 °C flash point) measured the flame spread rate about 2 – 20 mm/sec [9, 13, 14].

Unlike sub flash fuels, the flame spread rate over super flash fuels is significantly high. For instance the flame spread rate over fuels such as methanol, ethanol, and propanol measured to varies from 20 – 178 cm/sec [22, 23].

### **Temperature Distribution in Porous Bed**

Figures 11 and 12 illustrate the temperature distribution histories inside the porous beds made of 0.5 mm particle size. The depth of porous bed in Figure 11 is 26.6 mm, therefore the first set of thermocouples ( $Y = -1$  mm) were out of the sand bed. In this figure the variation of temperature in the porous bed is plotted versus elapsed time from the flame initiation. As shown in this figure the temperature of porous bed increases rapidly in all bed depths, the thermocouples locations, but the rate of increase slows down when the bed temperature approaches 82 °C which is very close to the boiling point of the fuel (82.4 °C). This phenomenon is referred to as temperature retardation. Beyond retardation, once again the temperature increases quickly to attain its maximum value.

Unlike Figure 11 in Figure 12, the temperature distribution was measured at three different depths namely;  $Y = -1$  mm,  $Y = -14.3$  mm and  $Y = -27.6$  mm from the bed surface, respectively. Comparison of the temperature distribution profiles in these two figures show that apart from the first set of thermocouples ( $Y = -1$ ) in these figures the temperature profiles at  $Y = -14.3$  mm and  $Y = -27.6$  mm are similar.

As shown in Figure 12, as the combustion proceeds the temperature increases to reach its maximum values. The maximum values for this bed was measured about 330, 200 and 130 °C at  $Y = -1$  mm,  $Y = -14.3$  mm and  $Y = -27.6$  mm from the bed surface, respectively. After that, the temperature declines gradually until the occurrence of spontaneous extinction. The obtained results for temperature distribution in this study are almost different from those observed by Kong et al [24]. The difference between the acquired results in this study and Kong study can be attributed to the quantity of fuel supply, as we used a finite quantity of liquid fuel compared with unlimited fuel supply in Kong's study. For the porous bed subjected to unlimited fuel supply, the flame burns like a pool fire. Thus at these types of beds as the combustion proceeds the fuel level goes down and turns from liquid phase to gas phase. This phase changing may have some impact on the temperature distribution profiles. Whereas in this study due to the limited quantity of liquid fuel the phase changing at the combustion zone is not that large.

The temperature retardation is observed at  $Y = -14.3$  and  $Y = -27.6$  mm between 700–1500 seconds after ignition (see Figure 12). The retardation points indicate the location at which the liquid fuel evaporation is completed. This implies that the region at which the temperature is higher than 82 °C is a dry region, as such, only fuel vapour exists at that region. According to the temperature histories recorded by thermocouples, the porous bed can be roughly divided into three regions, namely: (i) dry region located at the top and only contains fuel vapour, (ii) interface region, known as coexisting region and (3) liquid region (bottom layer). Figure 13 shows a schematic view of the locations of these regions.

As explained before by spreading the flame over the bed the fuel is gradually consumed and the fuel level turns from horizontal to parabolic form. The heat transferred from the flame to the porous bed increases the fuel temperature which increases the fuel evaporation rate. This creates a top region within the bed that is entirely vapoured. This region is located exactly under the porous bed surface and expands as the combustion proceeds. With the exception of dry region in the present study, which is due to the limited quantity of fuel supply, the acquired results for the other regions are agree very well with previous studies [1, 10, 11, and 24].

As observed in Figures 11 and 12 the porous bed temperature decreases as the bed depth increases. As shown the maximum temperature is related to the layers close to the surface. Equation 3 expresses that the bed maximum temperature is inversely proportional to the distance from the surface of bed.

$$T_{Max} \propto \frac{1}{Y} \tag{3}$$

Where  $T_{Max}$  is the maximum temperature and  $Y$  is the vertical distance from the surface (mm). This tendency is identical for all sorts of various particle sizes.

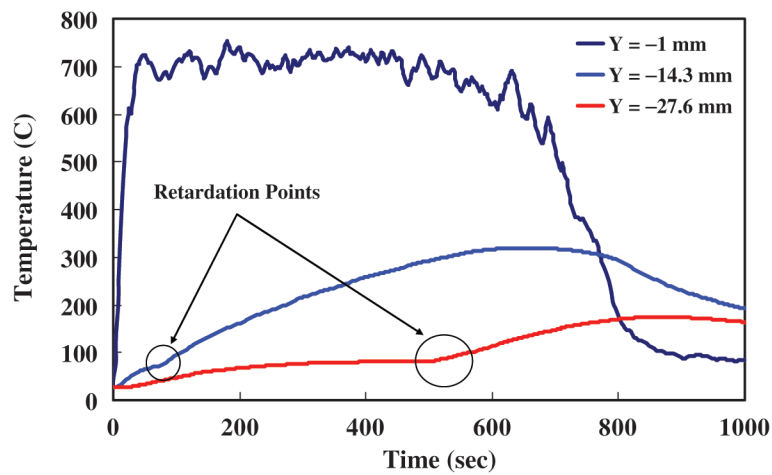


Figure 11. Temperature distribution profiles in the porous bed with mean particle diameters of 5 mm and a bed of 39.9 mm depth.

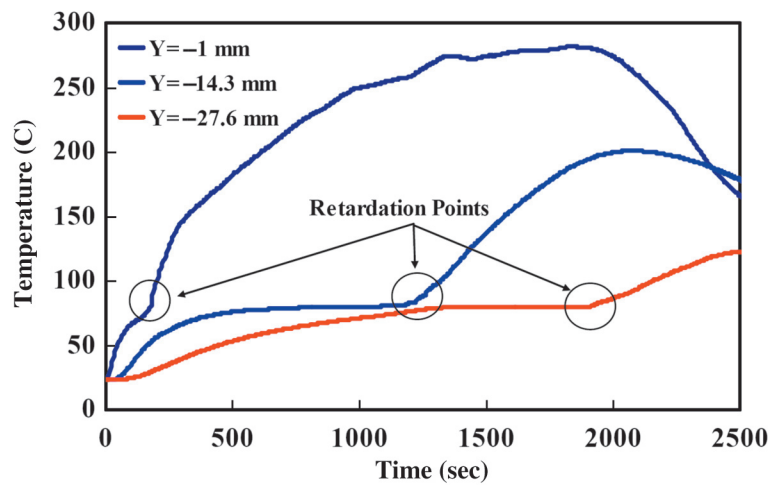


Figure 12. Temperature distribution profiles in the porous bed with mean particle diameters of 0.5 mm and a bed of 39.9 mm depth.

### Experimental Study of Temperature Distribution and Flame Spread Over an Inert Porous Bed Wetted with Liquid Fuel

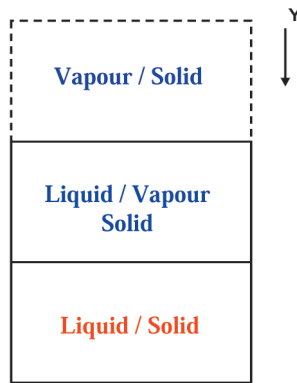


Figure 13. Schematic view of the liquid fuel different phases inside the porous bed.

### MODELING RESULTS

Figure 14 shows typical temperature distribution profiles in the porous bed predicted by solving Equation 1 and using parameters and values from Table 1. Figure 14 clearly indicates the existence of three distinct regions in the porous bed during the flame spread and combustion periods. As shown, the temperature at the first region is above  $77\text{ }^{\circ}\text{C}$  ( $350\text{ }^{\circ}\text{K}$ ), which is over the fuel boiling point. It indicates at this region only vapour exists.

At the second region located under the vapour region the temperature is between  $27\text{--}77\text{ }^{\circ}\text{C}$  ( $300\text{--}350\text{ }^{\circ}\text{K}$ ) which is around the boiling point  $82\text{ }^{\circ}\text{C}$  ( $355\text{ }^{\circ}\text{K}$ ) of the liquid fuel. This region generally contains both liquid and vapour fuel. It is usually called the co-existing region. The lowest region contains only liquid fuel. The temperature at this area is below  $27\text{ }^{\circ}\text{C}$  ( $300\text{ }^{\circ}\text{K}$ ). It is clearly observed that the predicted temperature profiles (see Figure 14) are in good agreement with the experimental results acquired in the present study (see Figures 11 and 12) and our previous studies [18, 19].

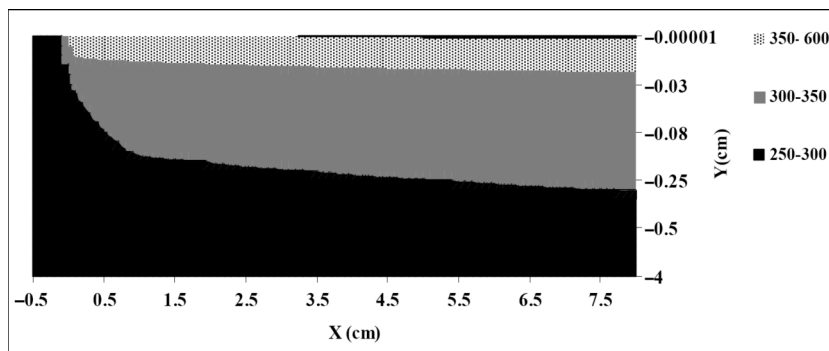


Figure 14. Temperature distribution profiles and region separation in the porous bed soaked with liquid fuel during the flame spread phenomenon; a) vapour region (top); b) Co-existing region (middle); c) liquid region (bottom).

### CONCLUSIONS

An experimental study has been carried out to investigate the flame spread rate and temperature distribution in the porous bed soaked with finite quantity supply of combustible liquid. The main conclusions derived from this study are as below;

The rate of flame spread in quiescent condition is much higher compared with flame spread under airflow condition.

Under both opposed and assisted airflow configurations the flame spread rate decreases as the air flow is increased although the decrease in the flame spread rate is more pronounced under opposed airflow. Similar flame deceleration behaviour is observed for deeper beds and larger bed particles.

Experimental and Predicted temperature distribution profiles show the existence of three distinctive regions; (vapour, vapour-liquid and liquid), in the porous bed which are formed during the flame spread and combustion phenomenon.

The flame leading edge is blue followed by yellow colour at the flame spreading stage. In addition as combustion proceeds the flame configuration turns to a conical shape, and attains to its maximum height about 0.3 m and 0.1 m under quiescent and 1.5 m/s assisted airflow, respectively.

#### ACKNOWLEDGEMENT

The authors wish to acknowledge the financial support provided to them by the University of Newcastle (Australia).

#### REFERENCES

1. Chao, CYH., Wang, JH. and Kong W, Effect of fuel properties on the combustion behaviour of different types of porous beds soaked with combustible liquid. *International Journal of Heat and Mass Transfer*, 2004. 47: p. 5201–5210.
2. Suzuki, T., et al. Flame spread over thin layers of crude oil sludge. In *Proceedings of the 1st International Symposium on combustion*. 1985. USA.
3. Suzuki, T. and Hirano, T. Flame propagation across a liquid fuel in an air stream. In *Proceedings of the 19th International Symposium on combustion*. 1982.
4. Ishida, H., Flame spread over fuel-soaked ground. *Fire safety Journal*, 1986. 10: p. 163–171.
5. Ishida, H., Flame spread over ground soaked with highly volatile liquid fuel. *Fire safety Journal*, 1988. 13: p. 115–123.
6. Ishida, H., Propagation of precursor flame tip in surrounding airflow along the ground soaked with high-volatile liquid fuel. *Journal of Fire Sciences*, 2005. 23: p. 247–259.
7. Ishida, H., Initiation of fire growth on fuel-soaked ground. *Fire Safety Journal*, 1992. 18(3): p. 213–230.
8. Ishida, H., Flame propagation in counter airflow along the ground soaked with highly-volatile liquid fuel, *Research report*. 2004: Japan.
9. Takeno, K. and Hirano, T. Flame spread over porous solids soaked with a combustible liquid. In *Proceedings of the 21st International Symposium on Combustion*. 1986.
10. Takeno, K. and Hirano, T. Behaviour of combustible liquid soaked in porous beds during flame spread. *Proceedings of the 22nd International Symposium on Combustion* 1988.
11. Takeuchi, T., et al. Burning characteristics of a combustible liquid soaked in porous beds. *Fire safety Science- Proceedings of the 3rd International Symposium*. 1991. UK.
12. Suzuki, T., Kawamata, M. and Hirano, T. Flame spread over fuel soaked sand in an opposed air stream. *Fire safety Science- Proceedings of the 2nd International Symposium*. 1989. Japan.
13. Suzuki, T., et al. Behaviour of the reverse flow in front of the leading flame edge spreading over fuel- soaked sand in an air stream. *Fire safety Science- Proceedings of the 3rd International Symposium*. 1991.
14. Suzuki, T., Kawamata, M. and Matsumoto, K. Aerodynamic and Thermal Structures of the leading Flame edge spreading over fuel soaked sand in an opposed air stream. *Proceeding in Thermal Engineering ASME/JSME*. 1991.
15. Wang, JH. and Chao, YHC. Combustion Behaviour of Liquid Fuel Soaked in Porous Beds, in *The 3rd Asia-Pacific Conference on Combustion*. 2001. p. 1–4.
16. Kong, W., Chao, YHC. and Wang JH. Behaviour of non-spread diffusion flames of combustible liquid soaked in porous beds. In *Proceedings of the 29th International Symposium on Combustion, 2002*
17. Kuwana, K., et al. Effect of liquid distribution on flame spread over porous solid soaked with combustible liquid. *Fire Safety Science, Proceedings of the 6th International Symposium*. 2000.
18. Zanganeh, J. and Moghtaderi, B. Flame spread under opposed and assisted airflow configurations over inclined porous beds soaked with combustible liquids. In *Fire Safety Science. Proceeding of the 9th International Symposium*. 2008. Germany.
19. Zanganeh, J. and Moghtaderi, B. Flame spread over a porous bed soaked with liquid fuel under assisted and opposed airflow condition. In *Proceedings of the 20th National and 9th International Conference of Heat and Mass Transfer, ISHMT-ASME*. 2010. Mumbai, India: .

20. Murphy, M.J. Flame spread rates over methanol fuel spills. *Combustion Science and Technology*, 1985. 42: p. 223–227.
21. Iijima, S., *Nature*, 1991. 354: p. 56–58.
22. Hirano, T., Suzuki, T. and Mashiko, I. Flame behaviour near steps bounding layered flammable mixtures. *In Proceedings of the 18th International Symposium on combustion*. 1981.
23. Ito, A., Masuda, D. and Saito, K. A Study of Flame Spread Over Alcohols Using Holographic Interferometry. *Combustion and Flame*, 1991. 83: p. 375–389.
24. Kong, W., Chao, CYH. and Wang, J. Burning characteristics of Non-spread diffusion flames of liquid fuel soaked in porous beds. *Journal of Fire Sciences*, 2002. 20(3): p. 203–224.
25. Torrance, K.E. and Mahjan, R.L. Fire spread over liquid fuels; liquid phase parameters. *In Proceeding of the 15<sup>th</sup> International Symposium on Combustion 1974*.
26. Torrance, K.E, Subsurface Flows Preceding Flame Spread Over a Liquid Fuel. *Combustion Science and Technology*, 1971. 3: p. 133–143.
27. Torrance, K.E. and Mahjan, R.L. Surface Tension Flows Induced by a Moving Thermal Source. *Combustion Science and Technology*, 1975. 10: p. 125–136.
28. Zanganeh, J. and Moghtaderi, B. Flame spread over porous sand and beds wetted with propenol. *Journal of Fire and Materials*, 2010.